

High p_T Hadron Spectra at High Rapidity

Ramiro Debbe† for the BRAHMS Collaboration

† Brookhaven National Laboratory, Upton NY, 11973

Abstract. We report the measurement of charged hadron production at different pseudo-rapidity values in deuteron+gold as well as proton-proton collisions at $\sqrt{s_{NN}} = 200\text{GeV}$ at RHIC. The nuclear modification factors R_{dAu} and R_{cp} are used to investigate new behaviors in the deuteron+gold system as function of rapidity and the centrality of the collisions respectively.

1. Introduction

The work reported in this presentation was motivated by the possibility of observing the onset of gluon saturation in d+Au collisions at RHIC. Saturation of the parton densities as their fractional longitudinal momenta x tends toward zero is widely accepted on the basis of hard limits set by unitarity (Froissart bound) [1], but the proper scale for that new regime, as well as its properties are the subject of intense study. Deep inelastic scattering of leptons on hadronic systems performed at HERA and FNAL have shown that for small- x values gluons are the dominant component of the hadron wave function and that their densities grow as powers of $\frac{1}{x}$ [2]. Limits to that growth have been proposed in a phenomenological description of the cross section of the virtual photon exchanged in those reactions. A functional form of that cross section is proposed such that it grows to become a constant beyond a scale that depends on x as $Q_s^2 \sim \frac{1}{x^\lambda}$ where $\lambda = 0.2 - 0.3$ is the only free parameter with values extracted from fits to data [3, 4]. A QCD based theory of dense partonic systems accessible with the new high energy colliders has been developed [5]. And the new regime it strives to describe is called the Color Glass Condensate (CGC). This theory offers a novel way of calculating nuclear properties at high energies based on classical field theory techniques.

The formalism of saturation can also describe p+A systems and the characteristic scale in transverse momentum is directly proportional to the density of partons in the ion: $Q_s^2 \sim \frac{A^{\frac{1}{3}}}{x^\lambda}$ and recalling the relation between the rapidity of a parton that carries the fraction x of longitudinal momentum and the rapidity of the hadron: $y_{parton} = y_{hadron} - \ln(\frac{1}{x})$ one can write $Q_s^2 \sim A^{\frac{1}{3}} e^{\lambda y}$. RHIC offers the advantage of combining high energy and high A ions (197 for gold) and BRAHMS, one of the four experiments currently collecting data at RHIC, can study particle production at high rapidity.

2. Experimental setup

The data presented in this report were collected with both BRAHMS spectrometers, the mid-rapidity spectrometer (MRS) and the front section of the forward spectrometer (FFS), complemented with an event characterization system used to determine the geometry of the collisions. A detailed description of the BRAHMS experimental setup can be found in [6]. However, the low multiplicity of charged particles in the proton or light ion reactions required an extension of the basic apparatus with a set of scintillator counters (called INEL detectors). These detectors [10] cover pseudo-rapidities in the range: $3.1 \leq |\eta| \leq 5.29$, and define a minimum biased trigger. This trigger is estimated to select $\approx 91\% \pm 3\%$ of the 2.4 barns d+Au inelastic cross section and $71\% \pm 5\%$ of the total inelastic proton-proton cross section of 41 mb. The INEL detector was also used to select events with collision vertex within ± 15 cm of the nominal collision point with a resolution of 5 cm.

The centrality of the collision was extracted from the multiplicity of the event measured within the angular region $|\eta| \leq 2.2$ with a combination of silicon and scintillator counters [7]. The results reported here were obtained without making use of the full complement of particle identification detectors. Ongoing analysis of the data includes particle identification and the use of the complete forward spectrometer FS.

3. Spectra

Experimental methods and analysis techniques used to extract the spectra presented here are described in [8]. Figure 1 shows the invariant yields obtained from p+p collisions (panel a) and d+Au collisions (panel b). For each system we studied particle production at 40 degrees with the MRS spectrometer and 12 and 4 degrees with the FFS spectrometer. Each distribution was obtained from several magnetic field settings and corrected for the spectrometer acceptance, tracking and trigger efficiency. No corrections were applied to the spectra for absorption or weak decays. Statistical errors are shown as vertical lines, and an overall systematic error of 15% is shown as shaded boxes on all points. The data points for the spectra extracted at $\eta = 3.2$ as well as those from $\eta = 2.2$ have been placed at the mean p_T calculated within each bin. This turns out to be equivalent in magnitude to the unfolding of the momentum resolution. The momentum resolution of the spectrometers at full magnetic field is $\delta p/p = 0.0077p$ for the MRS spectrometer and $\delta p/p = 0.0018p$ for the FS with p given in units of GeV/c. The p+p spectra have also been corrected for trigger efficiency by $13 \pm 5\%$ to make them minimum biased with respect to the total inelastic cross section. The proton+proton data sample at forward angles was collected in its majority with the magnets set to favor the detection of negative particles. The spectra at $\eta = 3.2$ have been fitted with a power law function $\frac{C}{(1+\frac{x}{p_0})^n}$ and the integral of that function over p_T^2 is compared for consistency in table 1 with UA5 results [9] for the p+p system, as well as our own multiplicity measurement for the d+Au system [10].

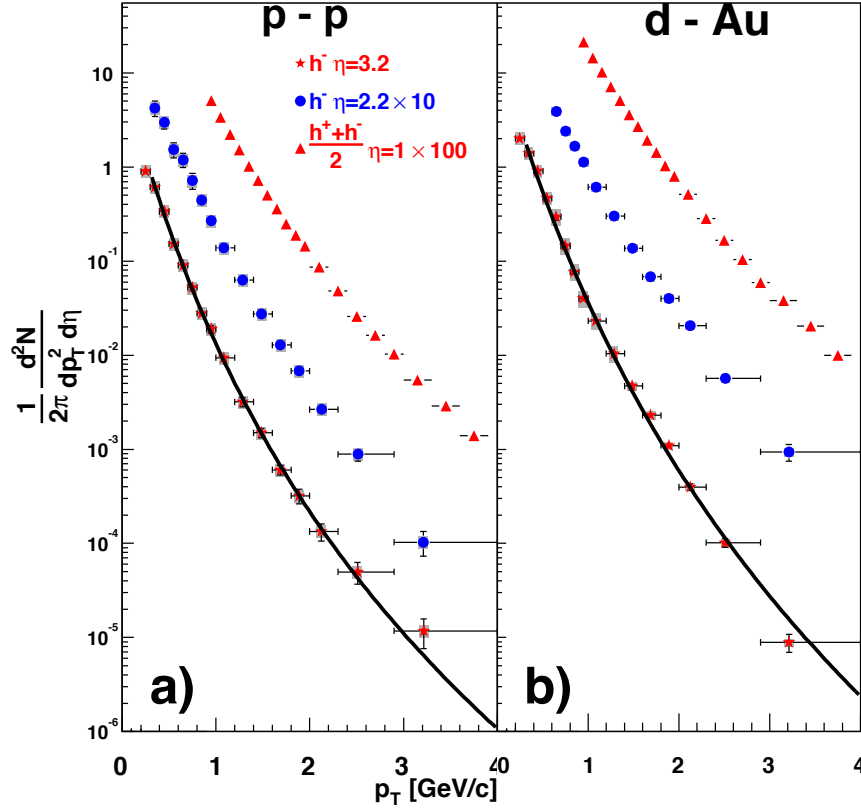


Figure 1. Spectra for charged hadrons at different pseudo-rapidities. Panel a shows the spectra obtained from proton-proton collisions and panel b those from d+Au collisions. The top most distributions in both panels correspond to the invariant yields of $\frac{h^+ + h^-}{2}$ measured at 40 degrees with the MRS spectrometer (scaled by 100 for clarity purposes), followed by the yields of negative hadrons measured at 12 (scaled up by 10) and 4 degrees respectively. The distributions obtained at $\eta = 2.2$ and 3.2 have variable bin size indicated by horizontal lines, the data points have been located at the mean value calculated within that particular bin. The distribution obtained at $\eta = 1$ has fixed bin width of 200 MeV/c and the data points are displayed at the middle of the bin.

Table 1. Fits to power law shapes at $\eta = 3.2$.

$System$	$\frac{dN}{d\eta}_{fit} / \frac{dN}{d\eta}_{meas}$	p_0	n	χ^2/NDF
$p + p$	$1.05 \pm 0.06 / 0.95 \pm 0.07$	1.18 ± 0.16	10.9 ± 0.9	13. / 11
$d + Au$	$2.23 \pm 0.09 / 2.1 \pm 0.6$	1.52 ± 0.1	12.3 ± 0.5	102 / 11

4. The nuclear modification factor

The d+Au spectra are compared to normalized p+p distributions measured at the same spectrometer setting. This comparison with p+p results is based in the assumption

that the production of moderately high transverse momentum particles scales with the number of binary collisions N_{coll} in the initial stages. The so called nuclear modification factor is defined as:

$$R_{dAu} \equiv \frac{1}{N_{coll}} \frac{N_{dAu}(p_T, \eta)}{N_{pp}(p_T, \eta)} \quad (1)$$

where N_{coll} is estimated to be equal to 7.2 ± 0.3 for minimum bias collisions.

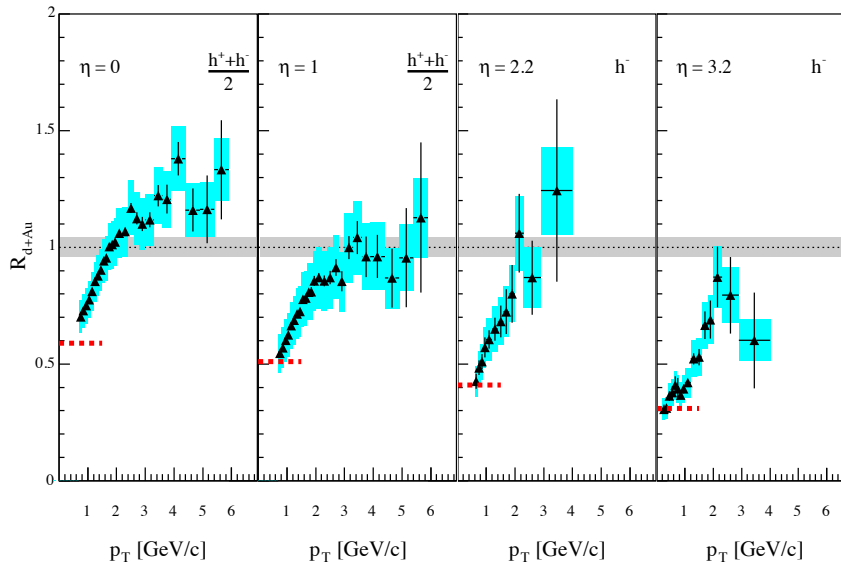


Figure 2. Nuclear modification factor for charged hadrons at pseudorapidities $\eta = 0, 1.0, 2.2, 3.2$. Statistical errors are shown with error bars. Systematic errors are shown with shaded boxes with widths set by the bin sizes. The shaded band around unity indicates the estimated error on the normalization to $\langle N_{coll} \rangle$. Dashed lines at $p_T < 1$ GeV/c show the normalized charged particle density ratio $\frac{1}{\langle N_{coll} \rangle} \frac{dN/d\eta(d+Au)}{dN/d\eta(pp)}$.

Figure 2 shows the nuclear modification factor defined above for four η values. The ratio at $\eta = 0$ and 1 was calculated by averaging on both positive and negative charges ($h^+ + h^-$)/2, and the one at $\eta = 2.2$ and 3.2 has been calculated including only h^- particles. The average charge is the preferred quantity because it compensates the isospin mismatches between the systems being compared. Because we do not have enough data to extract the distribution of positive charged particles from p+p, the ratio at $\eta = 2.2$ and 3.2 was calculated with spectra of negative charged particles. We can use the model PYTHIA to state that if we were to make the ratio with the average charge, the ratios would be smaller than those reported in this work. At mid-rapidity ($\eta = 0$), the nuclear modification factor exceeds 1 for transverse momenta with values greater than 2 GeV/c in similar way as the measurements performed by Cronin at lower energies [11]. Such enhancement has been related to multiple scattering at the partonic level [12].

Table 2. N_{part} and N_{coll} values extracted from HIJING calculations for d+Au collisions.

Centrality	$N_{part}(Au)$	$N_{part}(d)$	N_{coll}
Central 0 – 20%	12.5	1.96	13.6 ± 0.3
Semi – central 30 – 50%	7.36	1.79	7.9 ± 0.4
Peripheral 60 – 80%	3.16	1.39	3.3 ± 0.4

It is seen that a shift of one unit of rapidity is enough to make the Cronin type enhancement disappear, and further increases in η decrease even further the scaled yield of charged particles produced in d+Au collisions.

In all four panels, the statistical errors, shown as error bars (vertical lines), are dominant specially in our most forward measurements. Systematic errors are shown as shaded rectangles. An additional systematic error is introduced in the calculation of the number of collisions N_{coll} that scales the d+Au yields to a nucleon-nucleon system. That error is shown as a 15% band at $R_{dAu} = 1$.

We see a one to one correspondence between the R_{dAu} values at low p_T and the ratio $\frac{1}{\langle N_{coll} \rangle} \frac{dN/d\eta(d+Au)}{dN/d\eta(pp)}$ as demonstrated in Fig. 2 where that ratio is shown as dashed lines at $p_T < 1$.

5. Centrality dependence

The relation between particle yields and the centrality of the d+Au collision has also been explored using the fact that the multiplicity of charged particles in a reasonably wide η range ($|\eta| \leq 2.2$) correlates well to the impact parameter of the collision. Three samples of different centralities were defined according to the multiplicity of each event, and scaled histograms in transverse momentum were filled: $N_{central}(p_T) \equiv \frac{1}{N_{coll}} N_{0-20\%}(p_T)$ for events with multiplicities ranging from 0 to 20%. $N_{semi-central}(p_T) \equiv \frac{1}{N_{coll}} N_{30-50\%}(p_T)$ for semi-central events with multiplicities ranging from 30 to 50%, and finally, $N_{periph}(p_T) \equiv \frac{1}{N_{coll}} N_{60-80\%}(p_T)$ for peripheral events with multiplicities ranging from 60 to 80% with N_{coll} values listed in table 2.

With these histograms, two ratios were constructed: $R_{CP}^{central} = \frac{N_{central}(p_T)}{N_{periph}(p_T)}$ and $R_{CP}^{semi-central} = \frac{N_{semi-central}(p_T)}{N_{periph}(p_T)}$.

Because these ratios are constructed with events from the same data run, many corrections cancel out. The only correction that was applied to these ratios is related to trigger inefficiencies that become important in peripheral events. The dominant systematic error in these ratios stems from the determination of the average number of binary collisions in each centrality data sample. This error is shown as a shaded band around 1 in Fig. 3.

The four panels of figure 3 show the central $R_{CP}^{central}$ (filled symbols) and semi-central $R_{CP}^{semi-central}$ (open symbols) ratios for the for η settings. Starting on the left panel corresponding to $\eta = 0$, the central events yields are systematically higher than

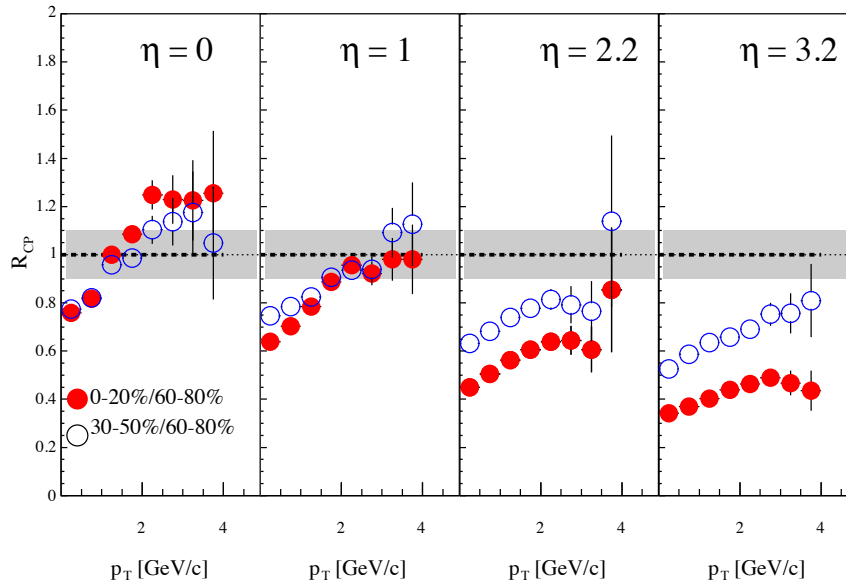


Figure 3. Central (full points) and semi-central (open points) R_{cp} ratios (see text for details) at pseudorapidities $\eta = 0, 1.0, 2.2, 3.2$. Systematic errors ($\sim 5\%$) are smaller than the symbols. The ratios at all pseudorapidities are calculated for the average charge $\frac{h^+ + h^-}{2}$.

those of the semi-central events. On the second panel corresponding to events measured at $\eta = 1$, the scaled yields of both samples are almost equal. At $\eta = 2$ the trend has already reversed, this time the semi-central events have higher yields than the central events, and finally, at $\eta = 3$, the yields of central events are $\sim 60\%$ lower than the semi-central events for all values of transverse momenta.

6. Discussion

The first results from the 2003 RHIC run showed that Cronin like enhancements are still prominent around mid-rapidity at RHIC energies and that jet suppression detected in Au-Au systems [13] is not present in d+Au [14, 8]. It was then concluded that jet suppression must happen in a medium formed after the interaction of the Au ions, and that medium is partonic and highly opaque.

In recent months, several groups reported theoretical discussions as well as numerical calculations within the context of the CGC with predictions about trends in the physics of deuteron-gold collisions at RHIC. Several authors showed that the color glass condensate exhibits a Cronin like enhancement at mid-rapidity [15, 16, 17, 18] while others argued for a gradual disappearance of such an enhancement as the energy of the collision or the rapidity of the measured particles is increased [19] or offered numerical calculations based on similar theoretical arguments [20]. All these theoretical works at higher rapidities introduce a modification of the gluon densities related to gluon emission

probabilities that grow as the rapidity gap between the probe and the target increases, within a formalism called ‘quantum evolution’. All these works predicted behaviors of the nuclear modification factor and its centrality dependence that are consistent with the measurements being reported in this paper.

However, other groups based their predictions and the description of the data with a two component model that includes a parametrization of perturbative QCD and string breaking as a mechanism to account for coherent soft particle production, the so called HIJING model [21]. Multiple scattering at the parton level has been added to this model with different degrees of sophistication and it describes well the d+Au results at mid-rapidity as well as the multiplicity densities that are dominated by soft processes. These models produce Cronin type enhancements at higher rapidities, and the magnitude of that enhancement grows with centrality. [22], [23]. Such behavior is not present in the data presented here.

More recently Miklos Gyulassy pointed the higher yield of positive charged particles at $\eta = 3.2$ shown in Fig 4 as ‘clear evidence of valence quark fragmentation’ [24] and the fact that the HIJING model provides a good representation of the data with a mechanism of string breaking introduced to explain low energy p-A measurements [25]. The authors of that paper offer an explanation for the triangular shape of the ratio $\frac{dN/d\eta(p+A)}{dN/d\eta(pp)}$ that is also present in these measurements.

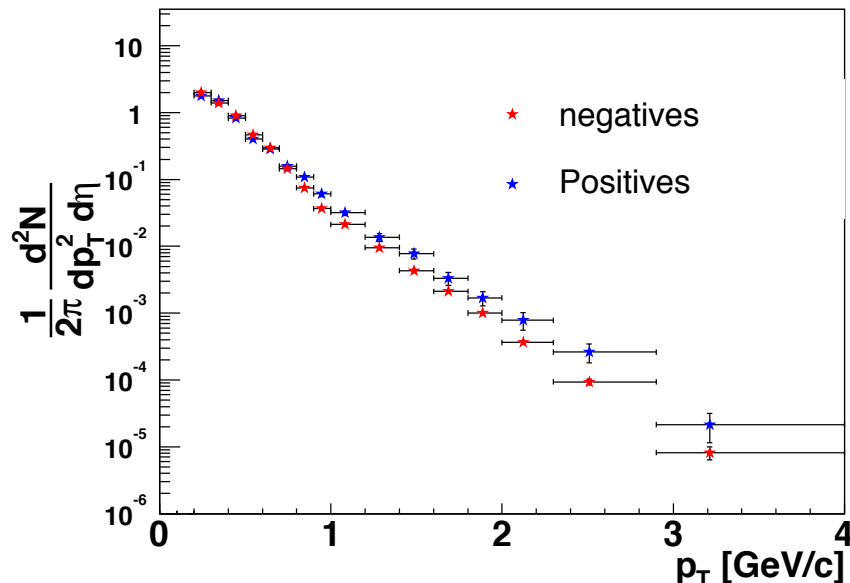


Figure 4. Spectra of positive and negative charged particles at $\eta = 3.2$

In summary, BRAHMS has studied the production of charged particles and compared their yields to those produced in proton-proton collisions scaled by the number of binary collisions and finds a clear evolution as the η of the particles changes from

mid-rapidity where a Cronin type enhancement is seen above transverse momentum of 2 GeV/c, to a gradual suppression as the values of η change to 1, 2.2 and 3.2. We have also found that the suppression increases with the centrality of the collision.

7. Acknowledgments

This work was supported by the Office of Nuclear Physics of the U.S. Department of Energy, the Danish Natural Science Research Council, the Research Council of Norway, the Polish State Committee for Scientific Research (KBN) and the Romanian Ministry of Research.

References

- [1] M. Froissart, Phys. Rev. **123** 1053 (1961).
- [2] J. Breitweg *et al.* Eur. Phys. J. C **7** 609-630, (1999); ZEUS Collaboration, J. Breitweg *et al.*, Phys. Lett. B **487** 53 (2000); ZEUS Collaboration, S. Chekanov *et al.*, Eur. Phys. J. C **21** 443 (2001); H1 Collaboration, C. Adloff *et al.*, Eur. Phys. J. C **21** 33 (2001).
- [3] Staśto A M, Golec-Biernat K, and Kwieciński J *Phys. Rev. Lett.* **86** 596-599 (2001).
- [4] Breitweg J *et al. Phys. Lett. B* **407**, 432 (1997).
- [5] L. McLerran and R. Venugopalan, Phys. Rev. D **49**, 2233 (1994), Phys. Rev. D **49**, 3352 (1994), Phys. Rev. D **50**, 2225 (1994), Phys. Rev. D **59**, 094002 (1999); Y. V. Kovchegov, Phys. Rev. D **54**, 5463 (1996), Phys. Rev. D **55**, 5445 (1997).
- [6] M. Adamczyk *et al.*, BRAHMS Collaboration, Nuclear Instruments and Methods A **499** 437 (2003).
- [7] Y.K. Lee *et al.*, Nuclear Instruments and Methods A **499** 437 (2003).
- [8] I. Arsene *et al.*, BRAHMS Collaboration, Phys. Rev. Lett. **91**, 072305 (2003).
- [9] G. J. Alner *et al.*, Z. Phys. C **33**, 1 (1986).
- [10] I. Arsene *et al.*, Submitted to Phys. Rev. Lett. ([nucl-ex/0401025](#));
- [11] D. Antreasyan *et al.*, Phys. Rev. D **19**, 764 (1979);
- [12] A. L. S. Angelis *et al.* Nucl. Phys. B **209**, 284 (1982).
- [13] K. Adcox *et al.*, PHENIX Collaboration, Phys. Rev. Lett. **88** 022301 (2002); S. S. Adler *et al.*, STAR Collaboration, Phys. Rev. Lett. **89** 202301 (2002); B.B. Back, *et al.*, PHOBOS Collaboration, Phys. Lett. B **578**, 297 (2004)
- [14] B.B. Back *et al.*, Phys. Rev. Lett. **91** 72302 (2003); S.S. Adler *et al.*, Phys. Rev. Lett. **91** 72303 (2003); J. Adams *et al.*, Phys. Rev. Lett. **91** 72304 (2003).
- [15] J. Jalilian-Marian, A. Kovner, A. Leonidov, H. Weigert, Phys. Rev. D **59**, 014014 (1999).
- [16] J. Jalilian-Marian *et al.* Phys. Lett. B **577**, 54-60 (2003), ([nucl-th/0307022](#)).
- [17] A. Dumitru and J. Jalilian-Marian, Phys. Lett. B **547**, 15 (2002)
- [18] Yu.V. Kovchegov, Phys. Rev. D **54**, 5463 (1996).
- [19] D. Kharzeev, Y. V. Kovchegov and K. Tuchin Phys. Rev. D **68**, 094013, (2003), ([hep-ph/0307037](#)); D. Kharzeev, E. Levin and L. McLerran, Phys. Lett. B **561**, 93 (2003).
- [20] R. Baier, A. Kovner and U. A. Wiedemann Phys. Rev. D **68**, 054009, (2003); J. Albacete, *et al.* ([hep-ph/0307179](#)).
- [21] X. N. Wang and M. Gyulassy, Phys. Rev. D **44**, 3501 (1991); M. Gyulassy and X. N. Wang, Comput. Phys. Commun. **83**, 307 (1994).
- [22] I. Vitev, Phys. Lett. B **562**, 36 (2003)
- [23] Xin-Nian Wang, Phys. Lett. B **565**, 116-122, (2003).
- [24] M. Gyulassy Proceedings RIKEN Workshop Volume **57**, 141 Dec. 2-6 (2003).
- [25] S. J. Brodsky, J. F. Gunion and J. H. Kuhn, Phys. Rev. Lett. **39**, 1120 (1977).